Air reverse circulation at the hole bottom in ice-core drilling

HU Zhengyi[1,2*], Talalay PAVEL[2*], ZHENG Zhichuan[2], CAO Pinlu[2], SHI Guitao[1], LI Yuansheng[1], FAN Xiaopeng[2], MA Hongmei[1]

[1]Key Laboratory for Polar Science of State Oceanic Administration,
Polar Research Institute of China, Shanghai, China

[2]Polar Research Center, Jilin University, Changchun, China

*Correspondence: Talalay Pavel (ptalalay@yahoo.com) and Hu Zhengyi (huzhengyi@pric.org.cn)

ABSTRACT. Ice-core drilling to depths of 200-300 m is an important part of research studies concerned with paleoclimate reconstruction and anthropogenic climate change. However, conventional drilling methods face difficulties due to firn permeability. We have developed an electromechanical ice-core drill with air reverse circulation at the hole bottom. We believe that the new drilling system will recover ice cores faster than shallow auger drills, with high efficiency and low energy consumption. The theoretically estimated up-hole speed of the airflow should be not less than 7.7 m s^{-1} to allow proper removal of ice cuttings from the borehole bottom. The computer simulation and test results showed that the design of the new ice-coring drill is feasible. The maximum allowed penetration rate depends by square law on airflow.

Keywords: ice coring; polar engineering; polar firn

1. INTRODUCTION

Ice-core drilling through snow/firn layers and solid ice to depths of 200-300 m is an important part of the International Partnerships on Ice Coring Sciences spatial 2000-year array (IPICS “2k Array”). This includes a network of ice-core climate and climate-forcing records for the last two millennia that can give answers about present and future climate change depending on natural climate variability. It is of great significance for research in geochemistry, microbiology, climatology and environmental science (Clow and Koci, 2002; Kawamura and others, 2003; Augustin and others, 2007; Johnson and others, 2007; Motoyama, 2007), and is of value for the development of human society

and understanding of the natural world. Dry drilling through firn is also a necessary preparatory step for intermediate and deep drilling with a drilling fluid.

To drill through upper permeable layers, cable-suspended electromechanical auger drills (so-called shallow drills) are usually used, in which cuttings are removed by auger conveyer to a chamber that is part of the drill (Talalay, 2016). The main feature of cable-suspended drills is that an armored cable with a winch is used instead of a drill pipe to provide power to the down-hole motor system and to retrieve the down-hole unit. Using a cable allows a significant reduction in power and equipment weight and can decrease the time required in round trip operations compared to pipe-based systems. During recent decades, shallow drills have become a very popular method of ice-core sampling. While some of them have performed very well, the main drawback is relatively short runs (typically, 1.0-1.2 m), and further development of shallow drilling systems remains an active issue today.

In search of new ways of shallow drilling and increasing drilling efficiency, we have developed an electromechanical drill with near-bottom air reverse circulation instead of auger conveying. Air drilling with direct airflow circulation in ice was first used in the mid-20th century on conventional drilling rigs (Kapitsa, 1958; Bazanov, 1961; Tongiorgi and others, 1962; Lange, 1973). Generally, the drilling performance was not stable, with several problems mainly related to the loss of circulation in the permeable snow/firn. Unless this zone is carefully walled off by casing, the airflow is insufficient to bring the cuttings up to the surface and they would thus remain in the borehole, possibly packing around the drill.

Similar complications were observed with the modern Rapid Air Movement (RAM) system that uses a flexible air hose to both suspend the drill and supply air at high pressure and high flow rates without casing (Bentley and others, 2009). It was found that firn permeability and conditions greatly restricted the depth to which it is possible to drill. In the 2010−2011 Antarctic field season, the drill could not reach depths below 63 m at the South Pole. To avoid airflow failure, Wang and others (2017) suggested using conventional reverse-circulation drilling technology with dual-wall drill rods in which compressed air flows downward through the annular space of the double-wall drill pipes and the inner tubes provide a continuous pathway for the chips and cores

from the coring head to the surface. However, all these drill rigs are still bulky, consume a lot of power and need a powerful air compressor to create enough air pressure for ice cuttings removal (Johnson and others, 2007).

One of the options to solve all the above-mentioned problems is to use an electromechanical ice-core drill with air reverse circulation where the cuttings are removed by near-bottom airflow into the chip chamber, along the same lines as the KEMS (Kudryashov and others, 1994) and IBED electromechanical drills (Talalay and others, 2017), but with the difference that the liquid pump is replaced by a blower. Here we present the concept, theoretical grounds, computer simulation and test results of this drilling method. The key target of the research was to prove the feasibility of the near-bottom air reverse circulation for firn/ice drilling. We expect the new drilling system to recover ice cores faster than shallow auger drills, with high efficiency and low energy consumption.

Power consumption to drive air impellers can be estimated according to:

$$N = pQ/\eta \quad (1)$$

where p is the pressure produced by the impeller; Q is the air flow; η is the efficiency. According to our estimations, the power consumption to drive air impellers is not less than 58 W, which is slightly less than the power required to transport ice cuttings by auger electromechanical drills (60-290 W, Talalay, 2003).

Simplification of some components (cable termination, instrumentation section) and the use of lightweight materials can significantly reduce the weight (<50 kg) and size of this type of the drill, allowing it to be delivered to a remote drill site by small aircraft or using sledges and backpacks.

2. GENERAL DESIGN OF THE DRILL

The upper part of the drill has the same components as other electromechanical drills (Fig. 1): cable termination to connect the drill with an armored cable; slip-ring device to prevent cable damage when the anti-torque fails; anti-torque system to prevent spinning of the non-rotating section; and pressure instrumentation chamber. The main new technical features of the drill are located in the lower part. There is one motor driving the core barrel with coring head, which is equipped with cutters and core catchers and the blower impellers through the planetary gear transmission. The coring

92 head cuts ice; and the blower produces a pressure difference that drives airflow and
93 removes ice cuttings during the drilling. The air flows through the drill head, ice core
94 barrel, chip chamber, blower impellers, and then into the space between the drill and
95 the borehole wall. The air forms air reverse circulation at the hole bottom, and the
96 underpressure inside the drill does not depend on the permeability of the drilled material.
97 The design of the chip chamber is quite complex. There is an annular clearance
98 between chip chamber and drill barrel. The air flows into the chip chamber through the
99 inlet of the chip chamber's inner tube. The top of the chip chamber is sealed, so the air
100 can only pass through the side filter screen. Ice cuttings are first moved by airflow to
101 the top of the chip chamber, then fall to the bottom under gravitational force.
102 Figure 1 near here
103 Key questions about the drill concept are whether circulation can be sustained at
104 the hole bottom and whether the circulating air can remove ice chips. It was therefore
105 decided to: research air reverse circulation in theoretical terms; set up an air reverse
106 circulation test stand to acquire some of the data required from the experiment in order
107 to prove that the air can form reverse circulation and readily suck ice cuttings into the
108 chip chamber; use the fluid dynamics software "Fluent 15", which is a general finite
109 element analysis (FEA) software developed by the ANSYS company, to verify the
110 parameters obtained from the theoretical calculation; and carry out the overall simulated
111 field trial after laboratory testing.

112 **3. THEORETICAL BACKGROUND**

113 Although air drilling has been used several times in glaciers and ice sheets, we are not
114 aware of any previous theoretical work on estimating air circulation parameters. The
115 following theoretical estimations aim to determine the minimum airflow speed required
116 for lifting ice cuttings from the hole bottom to the chip chamber.
117 Timely removal of ice cuttings is the first requirement. Cuttings are subjected to
118 gravitational force and air pressure when air flows through the cuttings surface. As the
119 air friction and air drag increase, the cuttings start to slide, roll and become suspended.
120 The airflow speed at that time is the critical shear speed for cuttings moving. Only when
121 airflow speed exceeds this critical shear speed are the cuttings likely to move (Nickling,
122 1988).

The airflow in the drill barrel is turbulent motion, so the ice cuttings are affected by several forces: head resistance or drag force, lifting force, impact force among ice cuttings and gravity.

The head resistance or drag force consists of: friction caused by relative motion between airflow and ice cuttings; and pressure difference between the windward and leeward of ice cuttings because of the vortex generated in the leeside of cuttings (Li and Zheng, 2003):

$$F_D = \frac{\pi}{8}\rho_g u_r^2 D^2 C_D \tag{2}$$

where F_D is the head resistance or drag force, u_r is relative speed between the airflow and the ice cuttings, ρ_g is the air density and D is the diameter of the cuttings. C_D is the resistance coefficient, which is shape dependent. For a flat cutting, C_D=1.4, for an angular or sub-circular cutting, C_D=0.85.

The lifting force is mainly caused by the shear of the rotation of cuttings and the airflow (Li and Zheng, 2003):

$$F_L = \frac{\pi}{8}\rho_g u_r D^3 \Omega \tag{3}$$

where F_L is the lifting force and Ω is the revolutions per second of the cuttings.

The impact force, the dominant force in the process of cuttings movement, is caused by collisions among cuttings according to the momentum conservation law:

$$\int_0^t F_m \mathrm{d}t = mu_2 - mu_1 \tag{4}$$

where F_m is the impact force, u_1 and u_2 are the speed of ice cuttings before and after collision.

According to Li and Zheng (2003), Bagnold proposed that the critical speed of moving particles, whose size exceeds 0.08 mm (Fletcher, 1976), may be given a semi-empirical formula, which has been derived through dimensional analysis and a series of experiments (Li and Zheng, 2003):

$$u_t = a\sqrt{(\rho_s/\rho_g - 1)gD} \tag{5}$$

where a is an empirical coefficient, g is gravitational acceleration, usually g = 9.8 m s^{-2}, and ρ_s is the cuttings density (kg m^{-3}).

The airflow speed during drilling can be obtained by:

$$u_g = 5.45k_s\left[\left(\rho_s/\rho_g - 1\right)gD\right]^{1/2}(1-\varphi_0)^{\beta} \quad (6)$$

where u_g is the minimum air delivery speed required for conveying cuttings (m s^{-1}), k_s is the conversion coefficient, generally 1.3–1.7 (dimensionless), φ_0 is the volume fraction of solid cuttings (dimensionless) and β is the test index, which is 2.3 when the Reynolds number is in the 10^3 - 2×10^5 range.

At steady state, the continuous supply of external energy ensures that the cuttings move at constant speed, which is called the final speed. Assuming that the moving particles are round, the ice cuttings' speed can eventually be calculated (Guo, 2006):

$$v_c = (1 + D_s/D_H)^{-1}\Psi\sqrt{\frac{4}{3}{C_D}^{-1}gD_s\left(\rho_s/\rho_g - 1\right)} \quad (7)$$

where v_c is the final speed of ice cuttings (m s^{-1}), D_s is the equivalent diameter of the ice cutting (m), Ψ is the sphericity coefficient (dimensionless) and D_H is the hydraulic diameter of the air (m).

According to the conservation of matter, the volume flow of ice cuttings in the channel is equal to the volume flow of ice chips produced by drilling. So, the chips' displacement speed can be calculated:

$$v_{tr} = \pi R_P D_b^2/14400AC_P \quad (8)$$

where v_{tr} is the air displacement speed (m s^{-1}), D_b is the hole diameter (m), C_P is the volume fraction of the ice cuttings in the stream (dimensionless), A is the cross-sectional area of the fluid (m^2) and R_P is the penetration depth per second (m s^{-1}).

The airflow speed required to carry the ice cuttings can be obtained by the following formula:

$$v_g = v_c + v_{tr} \quad (9)$$

where v_g is the airflow speed (m s^{-1}).

If it is supposed that the length of the ice chip chamber is 2 m, the central channel diameter of the air fluid is 40 mm, the inner and outer diameters are 115 mm and 125 mm, and the ice-core diameter is 100 mm, it can be calculated that u_g = 7.71 m s^{-1} and v_g= 8.24 m s^{-1} according to the (4)-(8). These numbers are quite close to the estimates of US drillers who indicated that an up-hole speed of approximately 7.62 m s^{-1} would be necessary to properly clean the hole of ice chips of approximately 2.54 mm diameter (Lange, 1973).

4. COMPUTER SIMULATION

In real ice-drilling conditions, the circulating air and cuttings constitute an air–solid two-phase flow model, considered as a continuous airflow, and the ice cuttings flow with the airflow. The ice cuttings cannot pass through the filter screen of the chip chamber with airflow (the mesh of the filter is 0.2 mm). To solve this problem numerically, a porous media model, which is a way of combining grid structured processing and unstructured processing, was created.

There is only approximate symmetry, so the model can be simplified, which can also reduce the computational load of the computer, as follows.

It is difficult to directly observe the pressure field and the speed field of the air in the full size picture, because the Length/Width ratio of the lower part of the drill is approximately 45:1. According to theoretical calculation and analysis, the airflow speed at the hole bottom is the key, and the pressure and speed fields in the straight tube are constant, so we just need to observe the pressure and speed fields near the head (A1 in Fig. 2), the junction of the core barrel and chip chamber (A2 in Fig. 2) and the top of the chip chamber (A3 in Fig. 2).

Figure 2 near here

The area of the windows on the drilling head (Fig. 3) controls the air velocity to lift the cuttings and should neither be too large, resulting in a lower air velocity, or too small which may cause a blockage of cuttings. The value h between the hole bottom and the cutters (Fig. 2) in the model calculations is a “trick” to simulate the effect of the windows, which cannot be precisely described in a model with axial symmetry. In practice there is no clearance between the hole bottom and the cutters when drilling. The distance h between the top surface of the drilling cutter and the hole bottom directly determines the suction capability of the blower. If h increases, the airflow speed near the bottom will decrease. Then, ice cuttings would be more difficult to remove from hole bottom. On the contrary, if the distance h decreases to a reasonable interval, ice cuttings will be picked up easily.

Figure 3 near here

In the simulation, h is assumed as 60 mm, the maximum value to pick all chips into chip chamber (Hu and others, 2012) and the vacuum degree is 20 kPa at first, around

the maximum value of used vacuum pump. The minimum airflow speed near the cutter can reach 25 m s^{-1}, which is sufficient to complete the task of sucking the ice cuttings during drilling. However, if the pressure difference is too large, there will be other drawbacks, e.g. core suffering from erosion due to air flow. Our premise is that the drilling work is smooth, as far as possible to reduce energy consumption and prolong the service life of the blower. So, in the next step we set several pressure differences (10 kPa, 9 kPa, …, 2 kPa, 1 kPa) and analyze the air velocity magnitude field near the coring head. With the pressure difference set to 3 kPa, the air velocity magnitude field near the cutters was solved by CFD and the results are shown in Fig. 4.

Figure 4 near here

Air speed as a function of distance from the center axis on the bottom plane of the coring head (line 1, Fig. 4) and the wall of the ice core (line 2, Fig. 4) were obtained. Furthermore, the speed as a function of distance from the center axis in the plane of the outlet and inlet are very important. The air speed as a function of distance from the center axis on these four planes is shown on Fig. 5.

Figure 5 near here

When the pressure difference is 3 kPa, the air speed along line 2 is just below 8.2 m s^{-1}. It means that the ice cuttings are produced slightly faster than ability of the air circulation. According to the simulation analysis of "Fluent" software, we can conclude that the final vacuum degree has a direct effect on the air flow rate and should be more than 3 kPa.

5. TESTS

In order to verify that the electromechanical ice-core drill with near-bottom air reverse circulation can work well and drill ice core smoothly, a test stand (Fig. 6) was constructed in Changchun City, Jilin Province, China, where the air temperature can reach -30 ℃ to -20 ℃ in winter. Such air temperatures can last for two months and create good conditions for simulating polar climate and ice drilling.

Figure 6 near here

In this experiment, artificial ice and lake ice were tested successively, and the artificial ice was frozen layer by layer. This experiment involves two main tests: an impeller test and a drilling test. In the impeller test, we changed different impellers in

244 the drill, and then increased the rotation speed of the output shaft. If the impellers were
245 not strong enough and produced insufficient underpressure, we changed them. The
246 better impellers were selected for use in the next test, which provides some test results.
247 First, the relationship between the rotation speed of the impellers and the final
248 vacuum was measured. We know of no suitable vacuum pump to install in the drill, so
249 blower impellers were chosen to produce the underpressure. The drill-driven motor was
250 connected with impellers through increasing planetary gears. The test results show that
251 the centrifugal impeller (Fig. 7a) works better than the axial flow impeller (Fig. 7b).
252 Figure 7 near here
253 Almost every relevant type of centrifugal impeller on the market were purchased
254 and tested (Fig. 7a and 7c), the parameters of these impellers shown in Table 1.
255 Table 1 near here
256 The findings from test were that the final vacuum degree is influenced by the
257 rotation speed, blade height impellers and impeller diameter. Final vacuum increases
258 with increasing rotation speed of the impellers when the impeller blade heights are
259 constant. In the same way, as long as the sealing is good, higher impellers blade and
260 larger impeller diameter yields greater vacuum degree. The underpressure generated by
261 #2 and #4 impellers can remove ice cuttings before they are twisted and damaged. The
262 underpressure generated by #1 impeller is insufficient with this gear increaser, and the
263 #3 impeller is twisted and damaged before it can produce sufficient vacuum degree (Fig.
264 6d).
265 With the #2 and #4 impellers, the relationship between vacuum degree and rotation
266 speed of the impellers is shown in Fig. 8.
267 Figure 8 near here
268 The vacuum degree produced by impeller #4 exceeds that of impeller #2 at the
269 same rotation speed, because the impeller blade height of impeller #4 is higher than that
270 of impeller #2. However, impeller #2 delivers a stronger vacuum if the rotation speed
271 reaches up to more than 20,000 rpm, in which impeller #4 will be damaged because of
272 high rotation speed. In the following experiments, impellers #2 were chosen as the
273 research object to obtain higher vacuum degree.
274 The fitted formula (Fig. 8) between vacuum degree without pressure loss y_{vd} (Pa)

and rotation speed x_{rs} (rpm) of the impeller can be obtained:

$$y_{vd} = 0.07x_{rs} - 442 \quad (10)$$

We then determined the relationship between the rotation speed of impellers and the penetration rate. Determining the minimum rotation speed of the impeller when the cuttings can be pumped completely under a different penetration rate provides a realistic basis for optimizing the drill design. Although we experienced setbacks and failures, e.g. ice cuttings sticking near the coring head (Fig. 9a) or insufficient impeller speed or sealing, we succeeded in many experiments (Fig. 9b and c).

Figure 9 near here

The data obtained by the measurement and control system showed the relationship between the impeller rotation speed and penetration rate (Fig. 10).

Figure 10 near here

The impeller rotation speed determines the maximum final vacuum, and using the regression results of vacuum versus rotation speed and penetration rate versus rotation speed, we obtain the equation of the penetration rate z_{pr} (m s^{-1}) and final vacuum degree y_{vd} (Pa):

$$z_{pr} = 0.02y_{vd} - 13.96 \quad (11)$$

There is a linear relationship between the airflow and the final vacuum. Therefore, the relationship between the airflow Q_{gf} (m^3 s^{-1}) and final vacuum degree (Liang and Xi, 2009) is given by

$$Q_{gf}{}^2 = 0.005y_{vd} - 0.7 \quad (12)$$

Finally, from (10)-(12) we derive the relationship between penetration rate and airflow:

$$z_{pr} = 4.2Q_{gf}{}^2 - 13.68 \quad (13)$$

6. CONCLUSIONS

Our study demonstrates that near-bottom air reverse circulation should theoretically be a sound option for polar ice core drilling. Air drilling systems can be relatively light and environmentally friendly. The maximal possible length of the coring run depends mainly on the design of the circulation system and capacity of the air blower. Theoretically estimated up-hole speed of the airflow should be not less than 7.7 m s^{-1},

which enables the proper removal of ice cuttings from the borehole bottom. The computer simulation and test results showed that the design of the ice-coring drill with air reverse circulation at the hole bottom is feasible. The maximum allowed penetration rate depends by square law on airflow. To drill faster and more safely, the number of impellers must be increased and their strength must be enhanced. Field tests will then be conducted in Antarctica as soon as financial and logistical support is obtained for the project.

ACKNOWLEDGEMENTS

We are grateful to our research team members for their help with the drill testing. This work was supported by grant No. 41327804 from the National Natural Science Foundation of China and the Program for Jilin University Science and Technology Innovative Research Team (Project No. 2017TD-24) the Fundamental Research Funds for the Central Universities. The authors thank Sune O. Rasmussen, Scientific Editor of Journal of Glaciology, Alex R. Pyne (Antarctic Research Centre, Victoria University of Wellington) and anonymous reviewers for fruitful discussion, useful comments and editing.

REFERENCES

Augustin L and 6 others (2007) Drilling comparison in 'warm ice' and drill design comparison. Annals of Glaciology, 47(1), 73-78.

Bazanov LD (1961) Opyt kolonkovogo bureniya na lednikakh Zemli Frantsa-Iosifa [Core drilling experiment on glaciers of Franz Josef Land]. Issledovaniya lednokov i lednikovikh raionov. Akademiya nauk SSSR. Institut Geografii. Mezhduvedomstvennyi Komitet po Provedeniiu MGG [Investigations of Glaciers and Polar Regions. Academy of Sciences of USSR. Interdepartmental Committee on Realization of International Geophysical Year]. Vol. 1, pp. 109–114 [In Russian].

Bentley CR and 12 others (2009) Ice drilling and coring. In: Drilling in Extreme Environments. Penetration and Sampling on Earth and other Planets. Y. Bar-Cohen, K. Zacny (Eds.). WILEY-VCH Verlag GmbH & Co., KGaA, Weinheim, pp. 221-308.

Clow GD and Koci B (2002) A fast mechanical-access drill for polar glaciology, paleoclimatology, geology, tectonics, and biology. Memoirs of National Institute of Polar Research Special Issue, 56, 5-37.

Fletcher B (1976) The interaction of shock with a dust deposit. Phys. D. Appl. Phys. 9, 197-202.

Guo B (2006). Air volume requirements for underbalanced drilling. China Petrochemical Press [In Chinese].

Hu Z, Talalay P, Cao P, Xue J, Zheng Z and Yu D (2012) Investigations of Near-Bottom Air Reverse Circulation in Non-Pipe Electromechanical Ice Drill Technology. Journal of Jilin University (Earth Science Edition) (s3), 374-378. (In Chinese)

Johnson J A and 7 others (2007) A new 122 mm electromechanical drill for deep ice-sheet coring (disc): 5. experience during greenland field testing. Annals of Glaciology, 47(1), 54-60.

Kapitsa AP (1958) Opyt bureniya l'da v Antarktide s ochistkoi zaboya vozdukhom [Experiment in ice drilling with removal of cuttings by air]. Burenie geologorazvedochnih skvazhin kolonkovim sposobom s ochistkoi zaboya vosdukhom [Prospect Core Drilling with Removal of Cuttings by Air]. Moscow, Gosgeoltechizdat, pp. 78–81. [In Russian]

Kawamura K, Nakazawa T, Aoki S, Sugawara S, Fujii Y and Watanabe O (2003) Atmospheric CO_2 variations over the last three glacial–interglacial climatic cycles deduced from the Dome Fuji deep ice core, Antarctica using a wet extraction technique. Tellus, 55(2), 126–137.

Kudryashov BB, Vasiliev NI and Talalay PG (1994) KEMS-112 electromechanical ice core drill. Memoirs of National Inst. of Polar Research, 49, 138-152.

Lange GR (1973) Deep rotary core drilling in ice. Cold Reg. Res. and Eng. Lab. Tech. Rep.; Hanover, United States, 94.

Li Z and Zheng B (2003) Mechanism of the Movement of Dust Particles. Blasting, 20(4), 17-19. [In Chinese].

Liang Z and Xi D (2009) Experimental study on air performance of household vacuum cleaner. Technical Papers (7), 48-50 [In Chinese].

Motoyama H (2007) The Second Deep Ice Coring Project at Dome Fuji, Antarctica. Scientific Drilling, 5(5), 67.

Nickling WG (1988) The initiation of particle movement by wind. Sedimentology, 35(3), 499-511.

Talalay P (2016) Mechanical Ice Drilling Technology. Springer Singapore.

Talalay PG (2003) Power consumption of deep ice electromechanical drills. Cold Regions Science and Technology, Vol. 37, 69-79.

Talalay P and 13 others (2017) Drilling project at Gamburtsev Subglacial Mountains, East Antarctica: recent progress and plans for the future. In: Siegert, M.J., Jamieson, S.S.R., White, D.A.

(Eds.) Exploration of Subsurface Antarctica: Uncovering Past Changes and Modern Processes. Geological Society, London, Special Publications, 461.

Tongiorgi E, Picciotto E, De BW, Norling T, Giot J and Pantanetti F (1962) Deep drilling at base roi baudouin, dronning maud land, antarctica. Journal of Glaciology, 4(31), 101-110.

Wang R and 6 others (2017) Rapid ice drilling with continual air transport of cuttings and cores: General concept. Polar Science, 14, 21-29.

List of figure captions:

Fig. 1. Schematic diagram of the drill with near-bottom air reverse circulation.

Fig. 2. The airflow field and the key observation sites. The model was divided into three parts to analyze the potential pressure weakest areas, lower part near the drilling head (A1), the junction part of the core barrel and chip chamber (A2) and the top part of chip chamber (A3). On the picture these parts are partitioned by vertical white break lines. The blue color indicates surrounding ice, the green color indicates air flow, the grey color indicates drill tube and the orange color indicates one part of chip chamber, which air cannot pass through. The upper drawing is a sketch of the core barrel and chip chamber shown as net, and the lower drawing shows circulation openings. While drilling, the air flows through windows in the coring head. However, in the two-dimensional model with rotational symmetry, this situation cannot be described exactly. In the model, *h* instead represents a distance equivalent to the area of the coring head windows.

Fig. 3. The drilling head. The green color on the two-dimensional model indicates the area of the windows, we can know that there are three windows from the geometry model.

Fig. 4. The air velocity magnitude field when the relative limit vacuum is 3 kPa.

Fig. 5. The speed as a function of distance from the center axis.

Fig. 6. Diagram of the testing platform.

Fig. 7. a, c) Centrifugal impeller; b) axial flow impeller; d) damaged impeller. As the rotation speed increased, the higher impeller blade twisted and damaged, like shown on Figure 7d.

Fig. 8. Relationship between vacuum degree and rotation speed of impeller.

Fig. 9. a-Ice cuttings pile up near the cutters; b-chip chamber filled with ice cuttings; c-ice core in core barrel.

Fig. 10. Relationship between impeller rotation speed and penetration rate.

397 Fig.1

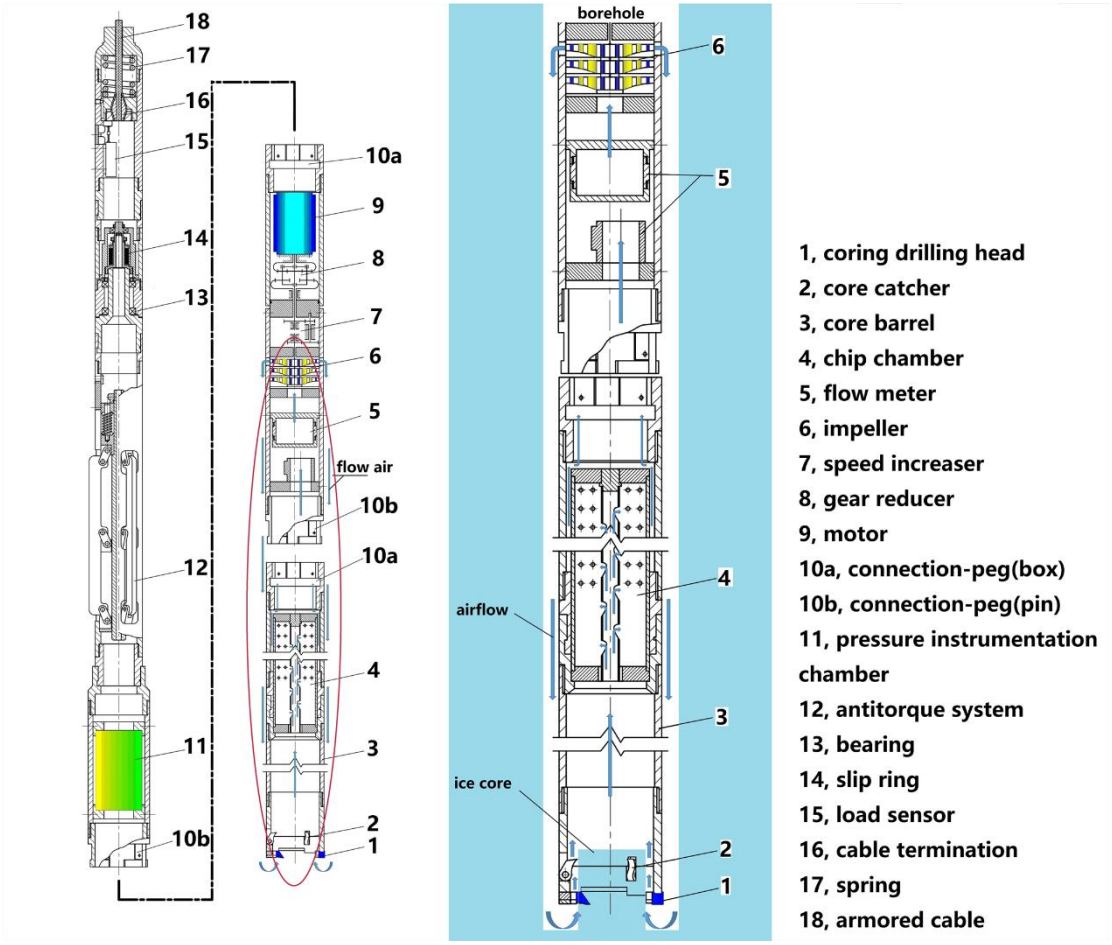
18
17
16
15
14
13
12
11
10b
10a
9
8
7
6
5
flow air
10b
10a
4
3
2
1
borehole
6
5
4
airflow
3
ice core
2
1
1, coring drilling head
2, core catcher
3, core barrel
4, chip chamber
5, flow meter
6, impeller
7, speed increaser
8, gear reducer
9, motor
10a, connection-peg(box)
10b, connection-peg(pin)
11, pressure instrumentation chamber
12, antitorque system
13, bearing
14, slip ring
15, load sensor
16, cable termination
17, spring
18, armored cable

398

399 Fig.2

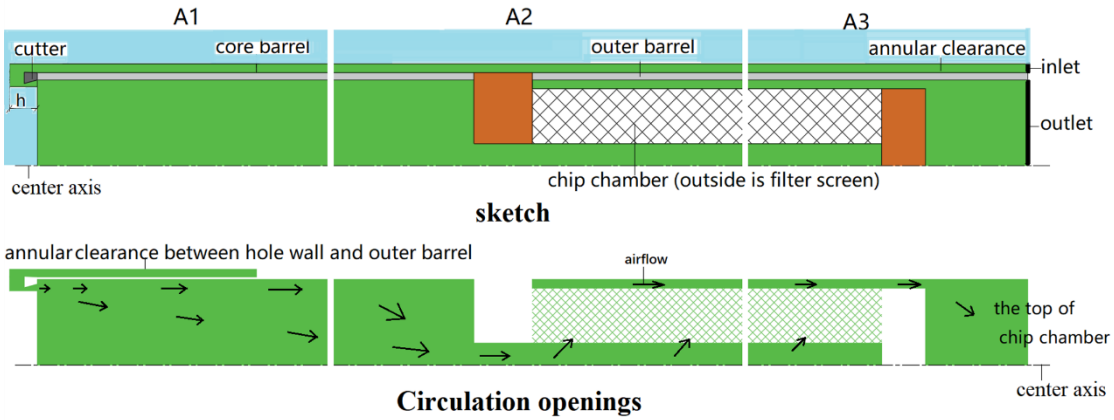
A1
A2
A3
cutter
core barrel
outer barrel
annular clearance
inlet
outlet
h
center axis
chip chamber (outside is filter screen)
sketch
annular clearance between hole wall and outer barrel
airflow
the top of
chip chamber
center axis
Circulation openings

400

401 Fig.3

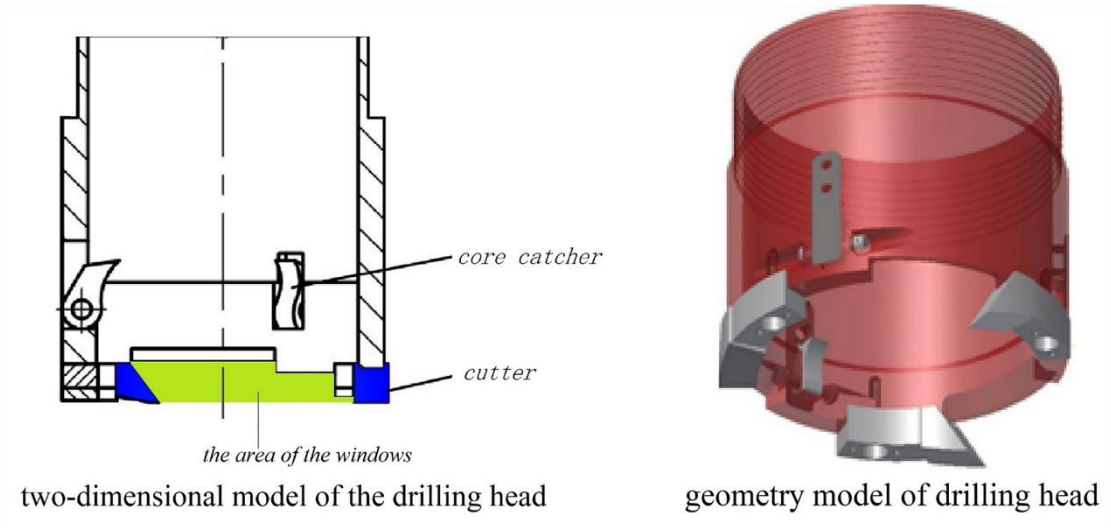

two-dimensional model of the drilling head

geometry model of drilling head

402

403 Fig.4

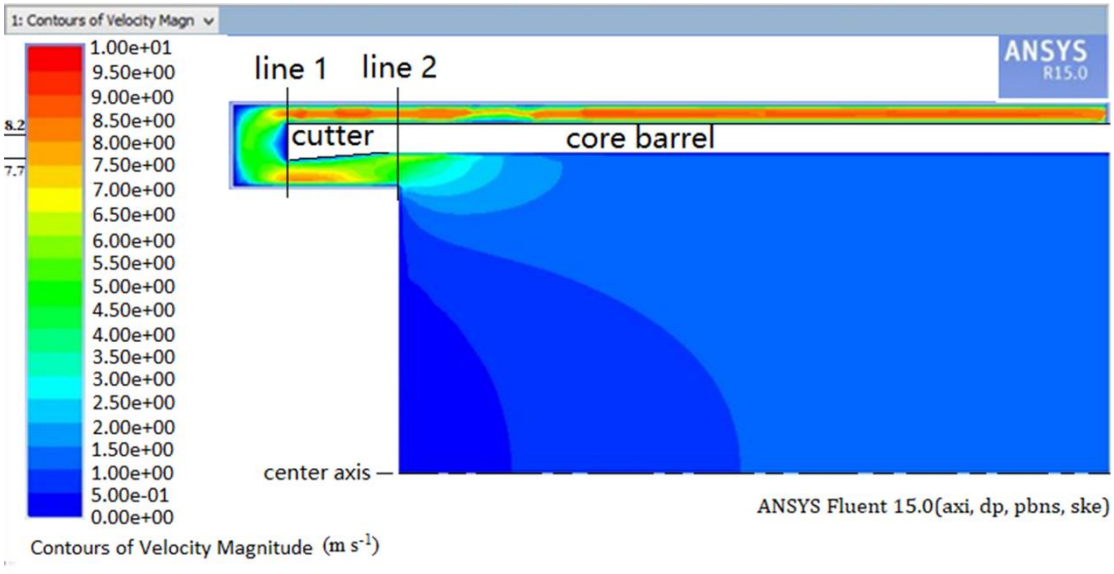
1: Contours of Velocity Magn
1.00e+01
9.50e+00
9.00e+00
8.50e+00
8.00e+00
7.50e+00
7.00e+00
6.50e+00
6.00e+00
5.50e+00
5.00e+00
4.50e+00
4.00e+00
3.50e+00
3.00e+00
2.50e+00
2.00e+00
1.50e+00
1.00e+00
5.00e-01
0.00e+00
Contours of Velocity Magnitude (m s-1)
line 1
line 2
cutter
core barrel
center axis
ANSYS
R15.0
ANSYS Fluent 15.0(axi, dp, pbns, ske)

404

405 Fig.5

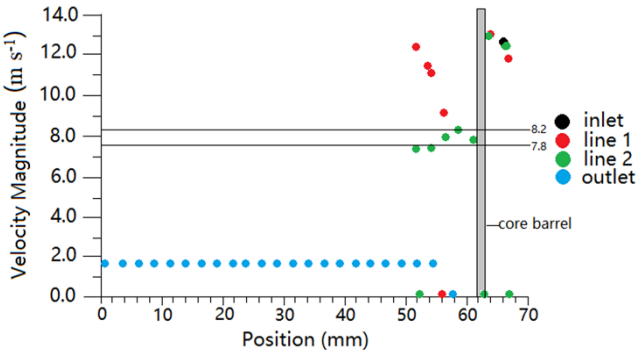
Velocity Magnitude (m s-1)
14.0
12.0
10.0
8.0
6.0
4.0
2.0
0.0
0
10
20
30
40
50
60
70
Position (mm)
8.2
7.8
core barrel
inlet
line 1
line 2
outlet

406

407 Fig.6

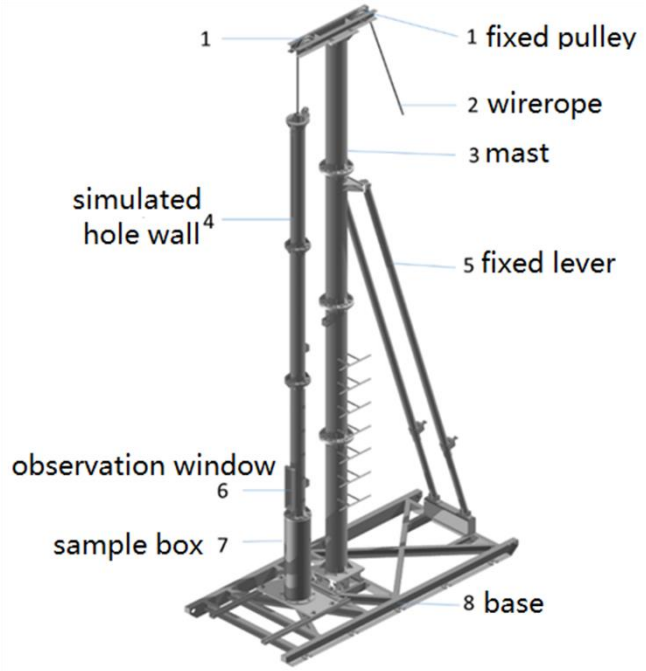
1
1 fixed pulley
2 wirerope
3 mast
simulated
hole wall 4
5 fixed lever
observation window
6
sample box 7
8 base

408

409 Fig.7

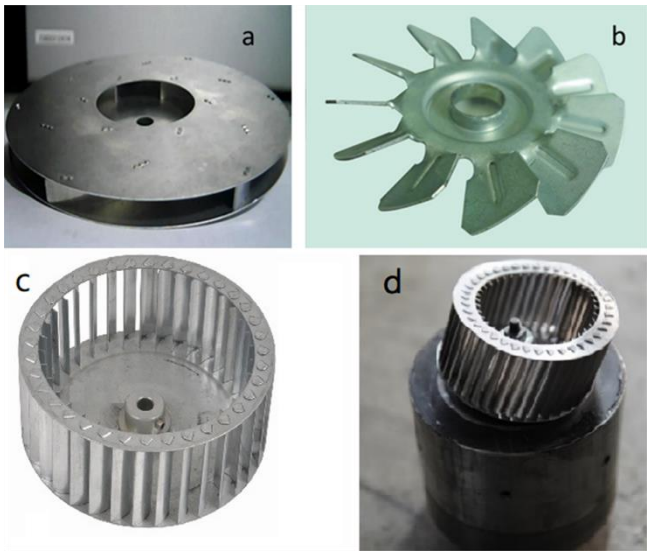

410

411 Fig.8

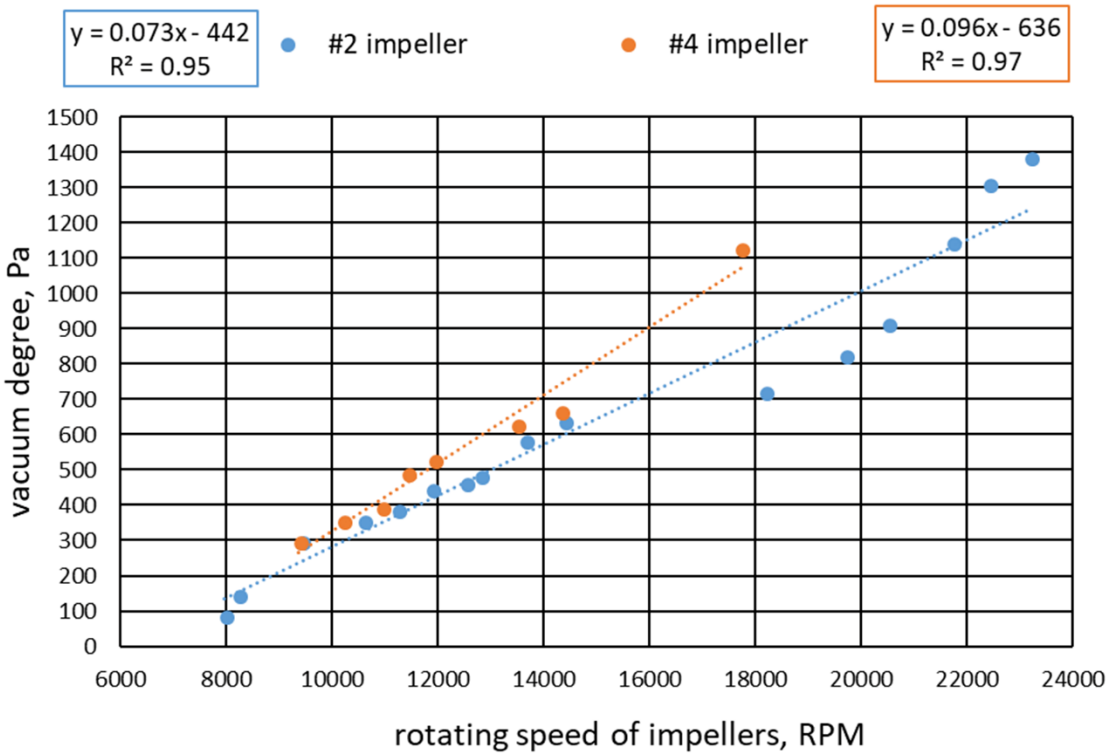
y = 0.073x - 442
R² = 0.95
#2 impeller
#4 impeller
y = 0.096x - 636
R² = 0.97
vacuum degree, Pa
1500
1400
1300
1200
1100
1000
900
800
700
600
500
400
300
200
100
0
6000
8000
10000
12000
14000
16000
18000
20000
22000
24000
rotating speed of impellers, RPM

412

413 Fig.9

414

415 Fig.10

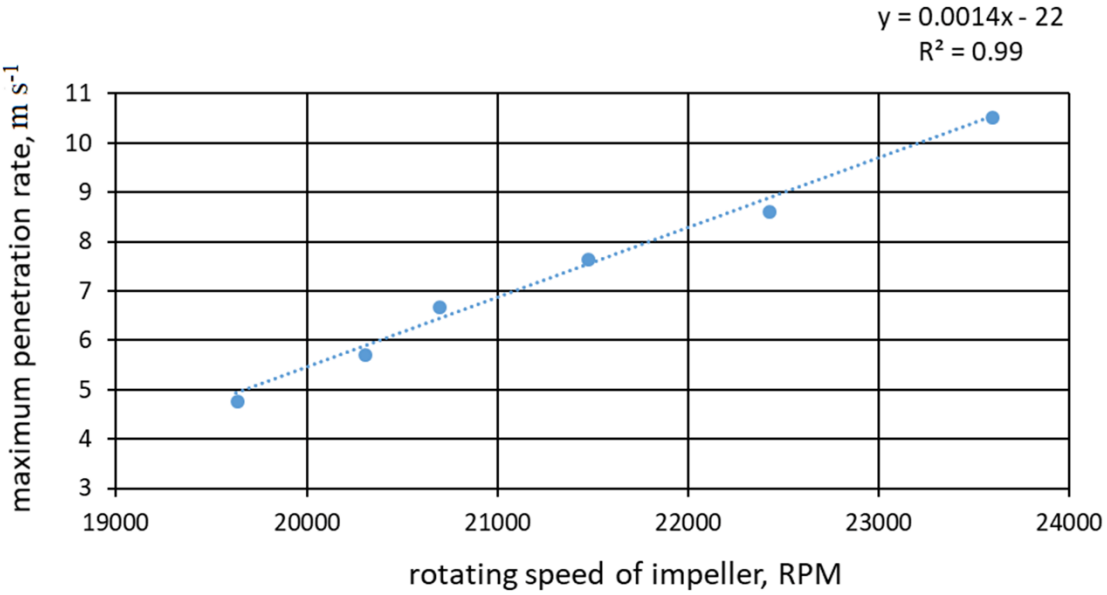

416

417 **Table 1**. Impeller parameters

Type		Outer Diameter (mm)	Number of blades	Inlet diameter (mm)	Blade height (mm)
a	#1	104	9	34.8	6.2-12.8
	#2	112			5.9-12
b	#3	84	24	54	30
			36		30
		85	45		34.1
			50		37.2
	#4	100	36	68	30

418